Development of a Novel Phase-Field Model for Fission Gas Bubble Swelling in UO_2 Nuclear Fuel

Changhyun Jo [a], Vishal Yadav [b], Michael R. Tonks [b], Youho Lee [a*]
a) *Department of Nuclear Eng., Seoul National Univ., 1 Gwanak-ro Gwanak-gu, Seoul 08826, Republic of Korea*
b) Department of Materials Science and Eng., Univ. of Florida, 100 Rhines Hall, Gainesville, FL 32611, United states
**Corresponding author: leeyouho@snu.ac.kr*

***Keywords : Phase-Field, Fission gas, UO_2, High burnup.**

1. Introduction

In response to nuclear industry's effort for burnup extension, fission gas release (FGR) has been intensively investigated due to its accelerated increase at high burnup. The primary objective in this field is to establish a framework that enhances the predictive capabilities for FGR under both steady-state and transient conditions within engineering-scale fuel performance codes, such as FAST, BISON, and GIFT [1]. This, in turn, demands a more robust mechanistic understanding at the meso-scale to enable effective upscaling to the engineering scale.

Phase-field modeling, a powerful numerical tool for simultaneously simulating mass transport and phase transformations, has been widely employed to investigate fission gas behavior in nuclear fuel. Previous models have primarily focused on the evolution of fission gas bubbles, often simplifying the bubble phase as a substitutional mixture of vacancies and gas atoms [2], [3]. However, a physical bubble is fundamentally a void pressurized by internal gas atoms. This physical discrepancy in existing models presents a significant limitation: the escape of gas atoms inherently triggers bubble shrinkage, failing to conserve the bubble volume.

In this study, we propose a novel phase-field method to simulate fission gas bubble swelling in UO_2 nuclear fuel. By modifying conserved variables and governing equations (Allen-Cahn and Cahn-Hilliard equations), we treat the bubble phase as a void filled with gas atoms (**Figure 1**). This approach enables the decoupling of gas atoms from vacancies within the bubble by implementing numerical source and sink terms at the phase interface. The proposed model offers advanced capabilities that distinguish it from previous works, specifically in accurately capturing bubble swelling under dilute vacancy concentrations and gas release to free surfaces.

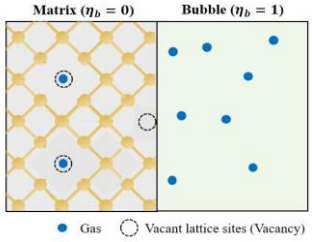

Figure 1 Schematic representation of fission gas behavior within UO2 matrix and bubble incorporated in this study.

2. Model Formulation

2.1. Variables and conserved fields

In phase-field modeling, the governing equations are formulated using continuous field variables, typically categorized into order parameters and concentrations. Since this model is implemented within a Finite Element Method (FEM) framework, the physical state of the domain is represented by these field variables defined across the computational mesh.

The current model incorporates one order parameter (η_b) and two concentrations for vacancies and gas atoms (c_v and c_g, respectively). This model encompasses two distinct phases: the bubble and the matrix. The order parameter (η_b), which is governed by the Allen-Cahn equation, identifies the local phase at any given point in the mesh, with values ranging from 0 to 1. Specifically, $\eta_b = 1$ corresponds to the bubble phase, $\eta_b = 0$ corresponds to the matrix, and $0 < \eta_b < 1$ denotes the diffuse interface between two phases.

The concentration fields quantitatively represent the two species (vacancies and gas atoms) present within the domain. Their evolution is governed by the Cahn-Hilliard equations, which involve the mass transport of the species throughout the system. Consistent with order parameter, both the vacancy and gas concentrations are defined as site fractions **(Eq.1)**, ensuring their values remain between 0 and 1.

$$(1)\ c_i = \frac{N_i}{N_{tot}}$$

where N_{tot} is the total number of available lattice sites within the matrix, N_i is the number of lattice sites occupied by i ($i = v\ or\ g$).

By definition, the vacancy concentration cannot be defined within the bubble, as the bubble itself is identified as a void formed by clustered and transformed vacancies. Thus, c_v is enforced to be zero within the bubble phase through the free energy density formulation, which is detailed in **Sec. 2.2**.

In a closed system without any source and sink terms, the total number of each species, calculated by integrating the concentration over the entire domain, must be conserved during mass transport. In this study, the gas is conserved across the domain **(Eq.2)** while a new conserved field ψ_2 is proposed in place of c_v alone.

Within the bubble, ψ_2 becomes unity, whereas it equals to $c_v + c_g$ within the matrix. This represents the concentration of vacant lattice sites devoid of U atoms within the matrix, including hidden vacancies coupled with the gas atoms.

$$(2)\ \psi_1 = c_g$$

$$(3)\ \psi_2 = \eta_b + c_v + (1-h)c_g$$

2.2. Free energy densities

The total free energy of the system (F) is calculated using **Eq. (4)**.

$$(4)\ F(\eta_b, c_v, c_g) = \int_v \left(f_{bulk}(\eta_b, c_v, c_g) + f_{int}(\eta_b)\right) dV$$

The bulk free energy density (f_{bulk}) accounts for the enthalpic and entropic changes associated with the chemical composition. To alleviate the computational burden arising from the logarithmic entropic term, the bulk free energies are often approximated by parabolic functions minimized at their equilibrium concentrations [2, 3]. Within matrix, the bulk free energy densities can be expressed as

$$(5)\ f_{bulk,v}^{mat} = \frac{1}{2}k_v^{mat}\left(c_v - c_{v,eq}^{mat}\right)^2$$

$$(6)\ f_{bulk,g}^{mat} = \frac{1}{2}k_g^{mat}\left(c_g - c_{g,eq}^{mat}\right)^2$$

where $c_{v,eq}^{mat}$ and $c_{g,eq}^{mat}$ are the vacancy and gas equilibrium concentrations in the matrix, respectively, and k_v^{mat} and k_g^{mat} are the parabolic coefficients: $k_v^{mat} = k_b T/(2V_a c_{v,eq}^{mat})$ and $k_g^{mat} = k_b T/(2V_a c_{g,eq}^{mat})$. V_a is the atomic volume of U in UO_2 and k_b and T correspond to the Boltzmann constant and the temperature, respectively.

Within the bubbles, the vacancy bulk free energy ($f_{bulk,v}^{bub}$) is expressed using an amplification factor $\mathcal{K}$ and $c_{v,eq}^{bub} = 0$. Thus, the parabolic coefficient of $f_{bulk,v}^{bub}$ becomes $\mathbb{K}k_v^{mat}$, which strongly enforces the vacancy concentration within bubble becoming zero. Gas bulk free energy density ($f_{bulk,g}^{bub}$) is represented by Van der Waals approach and also approximated by a parabolic form [4].

$$(7)\ f_{bulk,v}^{bub} = \frac{1}{2}\mathcal{K}k_v^{mat}(c_v - 0)^2$$

$$(8)\ f_{bulk,g}^{bub} = \frac{1}{2}A_{vdw}\left(c_g - c_{g,eq}^{bub}\right)^2$$

To calculate f_{bulk}, a two-step interpolation method, which interpolates the parabolic coefficients and the equilibrium concentrations separately, was employed to reduce the computational burden and induce a smooth transition across the interface [5].

$$(9)\ f_{bulk,v} = \frac{1}{2}[h\mathcal{K}\ k_v^{mat} + (1-h)k_v^{mat}]\left[c_v - (1-h)c_{v,eq}^{mat}\right]^2$$

$$(10)\ f_{bulk,g} = \frac{1}{2}\left[hA_{vdw} + (1-h)k_g^{mat}\right]\left[c_g - h(\eta_b)c_{g,eq}^{bub} - \left(1 - h(\eta_b)\right)c_{g,eq}^{mat}\right]^2$$

where $h = h(\eta_b) = \eta_b^3(6\eta_b^2 - 15\eta_b + 10)$ is a switching function. Therefore, f_{bulk} in **Eq. (4)** is calculated as the sum of $f_{bulk,v}$ and $f_{bulk,g}$.

The interfacial free energy density (f_{int}) arises from the atomic disorder at the phase interface. This is composed of the double-well potential and a gradient energy density, while maintaining the consistency with macroscopic interfacial energy (γ).

$$(11)\ f_{int} = W\eta_b^2(1-\eta_b)^2 + \frac{\kappa_\eta}{2}(\nabla\eta_b)^2$$

$$(12)\ \int_{\delta_{int}} f_{int}\, dx = \gamma$$

where W is the height of the double well potential, κ_η is the gradient potential coefficient, δ_{int} is the interfacial thickness.

2.3. Governing equations

This model employs three governing equations (**Eqs. (13)-(15)**) to describe the phase transformation and mass transport. Notably, the evolution of the concentration fields is dervied from the Cahn-Hilliard for the conserved fields ψ_i ,defined as $\dot{\psi}_i = \nabla \cdot \left(M_i \nabla(\delta F^*/\delta\psi_i)\right)$ for $F^*(\eta_b, c_g, c_v) = F(\eta_b, c_g, \psi_2)$:

$$(13)\ \dot{\eta_b} = -L_\eta\left(\frac{\delta F}{\delta \eta} + (h' c_g - 1)\frac{\delta F}{\delta c_v}\right)$$

$$(14)\ \dot{c_g} = \nabla \cdot \left(M_g \nabla\left(\frac{\delta F}{\delta c_g} - (1-h)\frac{\delta F}{\delta c_v}\right)\right)$$

$$(15)\ \dot{c_v} = \nabla \cdot \left(M_v \nabla \frac{\delta F}{\delta c_v}\right) - (1-h)\dot{c_g} + \left(h' c_g - 1\right)\dot{\eta_b}$$

where L_η is the Allen-Cahn mobility for η_b. The parameters $M_1 = M_v = D_v/(\partial^2 f_{bulk}^{mat}/\partial c_v^2) = D_v/k_v^{mat}$ and $M_2 = M_g = D_g/(\partial^2 f_{bulk}^{mat}/\partial c_g^2) = D_v/k_g^{mat}$ are the Cahn-Hilliard mobility for c_v and c_g respectively, which are expressed in terms of vacancy diffusion coefficient (D_v) and the gas diffusion coefficient (D_g). This formulation ensures the conservation of both two fields in **Eq. (2) and (3)** for a closed system.

During computation, a normalized vacancy concentration ($\tilde{c_v} = c_v/c_{v,eq}^{mat}$) is practically used instead of c_v to minimize floating-point errors. In the previous studies which treated the bubble phase as a mixture where $c_{v,eq}^{bub} \cong 0.55$ (i.e. $c_{v,eq}^{bub}/c_{v,eq}^{mat} \cong 10^4 - 10^5$),

utilizing $\tilde{c}_v$ for computation was practically impossible due to this massive discontinuity.

In the proposed phase-field model, the quantification of key modeling parameters was systematically conducted to balance physical accuracy with numerical stability. The gradient energy coefficient ($\kappa_\eta = 100$ eV/nm) and the double-well potential height ($W = 9.60$ eV/nm^3) were calibrated to ensure that the integrated energy density across the diffuse interface accurately matched the experimentally measured macroscopic interfacial energy of $\gamma = 7.302$ eV/nm^2.

To strictly enforce the physical constraint of zero vacancy concentration inside the bubble phase without causing excessive computational overhead, the parabolic amplification factor for vacancies ($\mathcal{K}$) was set to 100. Furthermore, the Allen-Cahn mobility (L_η) was quantified by analyzing total free energy curves over time to guarantee that the overall phase transformation kinetics remained within a strictly diffusion-controlled regime, leading to an adopted value of 1.0×10^{-6} nm^3/eV/s.

3. Result and discussion

To evaluate the effect of incorporating the physical concept of the bubble phase into the model, the proposed model was quantitatively compared against a previous model under two specific 2D case. The previous model is based on the Grand Potential approach [3], where the equilibrium concentration of vacancy is 0.55 and that of gas atoms is 0.45, implying that the bubble phase was treated as substitutional mixture devoide of U atoms. All formulations and material properties were kept identical for both models, except for the vacancy free energy in the bubble.

3.1. Swelling under dilute vacancy concentration

Figure 2 shows a geometric illustration of the simulated condition for bubble swelling under dilute vacancy concentration. The bubble initially started with a radius of 80 nm and an interfacial thickness of 20 nm within a 400 x 400 nm^2 domain. Within the bubble, c_v and c_g were initialized at their respective equilibrium concentrations, whereas within the matrix, they were set to 1.5 times their equilibrium concentrations. Additionally, at the boundaries, c_v and c_g were fixed at 1.5 times their equilibrium concentrations, acting as sources that continuously providing vacancies and gas atoms into the domain. During the simulation, the domain was adaptively discretized, ensuring that the finest mesh size was 1 x 1 nm^2.

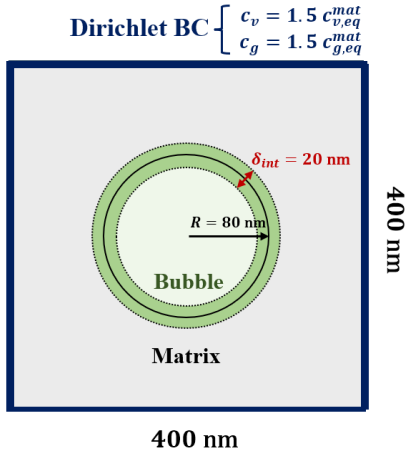

Figure 2 Geometric illustration of the simulated condition for swelling under dilute vacancy concentration.

As shown in **Figure 3**, our model showed that the bubble consistently swells while consuming vacancies under the dilute vacancy concentration. In contrast, the previous model exhibited bubble shrinkage rather than the swelling. This behavior primarily arises from an inherent limitation of the previous models, which cannot mitigate floating-point errors due to the massive difference in the equilibrium concentrations between the matrix and the bubble.

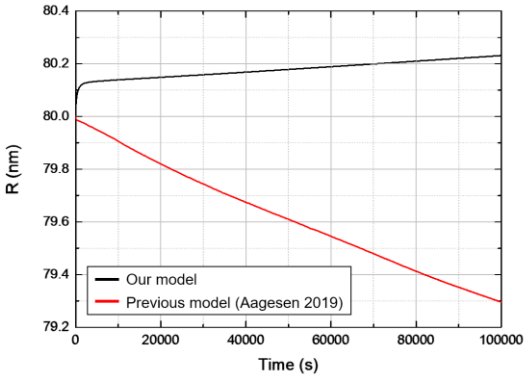

Figure 3 Comparison of temporal evolution of the bubble radius simulated using the proposed model and the previous model.

3.2. Fission gas release through free surface

Figure 4 demonstrates the geometrical condition to simulate fission gas release through free surface. A bubble with identical size used in **Sec. 3.1** was attached on the right boundary of the domain (400 x 300 nm^2), which acts as a free surface.

Since the free surface acts as a both sink and source term for vacancies and only a sink term for gas atoms, this was numerically implemented by fixing the concentrations at the boundary as follows: (i) $c_v = hc_{v,eq}^{mat} + (1-h)c_{v,eq}^{bub}$, (ii) $c_g = 0$. Thus, it was supposed

to confirm the behavior of how gas atoms escape from the bubble while vacancy movement is limited.

The other three boundaries were set up with a Neumann Boundary Condition, enforcing no outward flux. c_v and c_g were initialized to be their equilibrium concentrations both within the bubble and the matrix. The simulation was conducted with the finest mesh size of 1 x 1 nm^2.

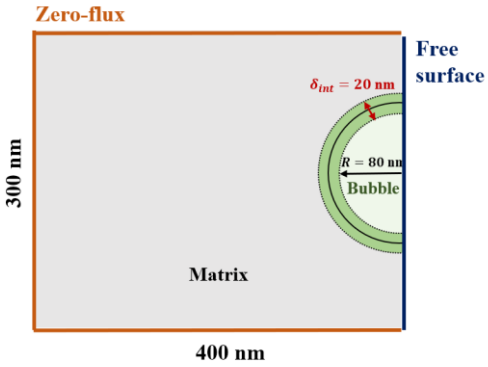

Figure 4 Geometrical illustration of the simulated condition for fission gas release through free surface.

Figure 5 shows the temporal evolution of average gas flux on the right boundary of the domain. As the gas free energies were identically applied within both models, they started at the same initial value of gas flux. As the gas concentration within the bubble became depleted, our model exhibited a gradually decreasing trend while the previous model estimated an abrupt decrease in the gas flux.

This is primarily due to a physical discrepancy in the previous model assuming the bubble as a substitutional phase. In the previous model, as gas atoms escaped from the bubble, they left behind vacant lattice sites, causing the bubble shrinks and detached from the free surface. This resulted in gas trapping behavior, as shown in **Figure 6**. This observation underscores our model's capability to provide reliable results regarding gas release at the free surface, particularly by decoupling the gas atoms from vacancies within the bubble.

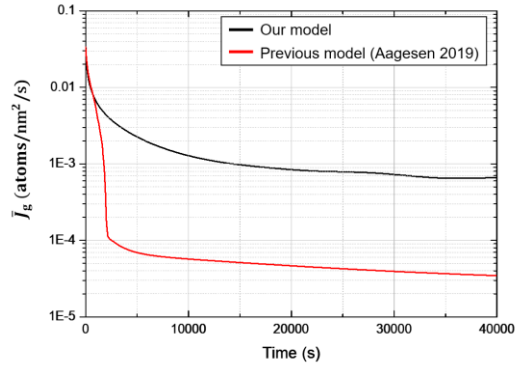

Figure 5 Comparison of temporal evolution of average gas flux on the right boundary (Free surface), simulated through our model and the previous model.

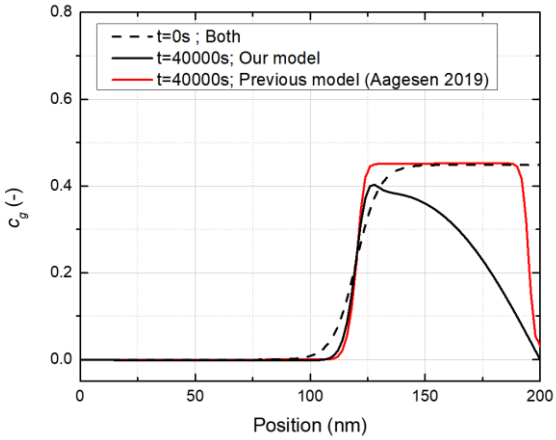

Figure 6 Comparison of spatial distribution of gas concentration along the center horizontal line (y=0), simulated through our model and the previous model.

4. Conclusion

We have developed a novel phase-field method to simulate the fission gas bubble swelling in UO_2 nuclear fuel. This model includes the physical representation of the bubble as a void pressurized with gas atoms, resolving major limitations of the previous models such as treating dilute vacancy concentrations and decoupling gas-vacancy behavior within bubble. This implies that the developed model could be utilized to improve the mechanistic understanding of fission gas release particularly at high burnup, thereby mitigating the substantial uncertainties that currently exist.

Acknowledgement

This work was supported by the Korea Institute of Energy Technology Evaluation and Planning(KETEP) and the Ministry of Climate, Energy & Environment(MCEE) of the Republic of Korea (No. RS-2025-02633904, Center for Advanced Nuclear Fuel Innovation).

REFERENCES

[1] K. Shim, H. Rho, C. Lee, C. Jo, and Y. Lee, "GIFT-1.0: Advanced light water reactor fuel performance code," *Nucl. Eng. Technol.*, vol. 57, no. 9, p. 103567, Sep. 2025, doi: 10.1016/j.net.2025.103567.

[2] L. K. Aagesen, S. Biswas, W. Jiang, D. Andersson, M. W. D. Cooper, and C. Matthews, "Phase-field simulations of fission gas bubbles in high burnup UO 2 during steady-state and LOCA transient conditions," *J. Nucl. Mater.*, vol. 557, p. 153267, Dec. 2021, doi: 10.1016/j.jnucmat.2021.153267.

[3] L. K. Aagesen, D. Schwen, M. R. Tonks, and Y. Zhang, "Phase-field modeling of fission gas bubble growth on grain boundaries and triple junctions in UO2 nuclear fuel," *Comput. Mater. Sci.*, vol. 161, pp. 35–45, Apr. 2019, doi: 10.1016/j.commatsci.2019.01.019.

[4] J. D. van der Waals, *Over de continuïteit van den gas- en vloeistoftoestand*. Sijthoff, 1873.

[5] B. Dabas, A. Ruffini, Y. Le Bouar, T. Jourdan, and A. Finel, "Phase-field modeling of cavity growth and dislocation climb," *Acta Mater.*, vol. 293, p. 121040, Jul. 2025, doi: 10.1016/j.actamat.2025.121040.